

Original Research Article

Investigating the Strength and Chloride Corrosion Resistance of Steel Pipes Coated with Combretum Combretaceae Exudates

Charles Kennedy^{1*}, Kanee Sorbari²

¹School of Engineering, Department of Civil Engineering, Kenule Beeson Saro-Wiwa Polytechnic, Bori, Rivers State, Nigeria

²School of Engineering, Department of Mechanical Engineering, Kenule Beeson Saro-Wiwa Polytechnic, Bori, Rivers State, Nigeria

***Corresponding Author:** Charles Kennedy

School of Engineering, Department of Civil Engineering, Kenule Beeson Saro-Wiwa Polytechnic, Bori, Rivers State, Nigeria

Article History

Received: 04.06.2025

Accepted: 11.07.2025

Published: 14.07.2025

Abstract: This study investigates the effectiveness of Combretum Combretaceae exudates as a natural coating aimed at enhancing both the strength and chloride corrosion resistance of steel pipes. Corrosion, particularly chloride-induced corrosion, presents significant challenges across various industries, including oil and gas, water supply, and infrastructure, leading to substantial economic losses estimated at over \$300 billion annually in the U.S. alone. It poses severe safety risks, necessitating the urgent need for effective and environmentally responsible corrosion management strategies. Traditional corrosion protection methods, such as synthetic coatings and galvanization, often rely on harmful chemicals that can have detrimental environmental impacts. This scenario underscores the importance of exploring eco-friendly alternatives that do not compromise protective efficacy. The research presented herein demonstrates that steel pipes coated with Combretum exudates exhibit markedly improved corrosion resistance, evidenced by a reduction in corrosion rates of up to 98.6% compared to uncoated samples. This substantial decrease in corrosion rates highlights the potential of natural coatings in mitigating the adverse effects of corrosive environments. Mechanical testing further reveals that these coatings effectively preserve key mechanical properties, including tensile and yield strength, mitigating degradation over extended exposure periods of up to 210 days. Specifically, coated samples retained 91% of their original tensile strength and 89% of their yield strength, demonstrating the coatings' ability to provide robust protection against corrosion while maintaining the structural integrity of the steel. The study establishes a clear relationship between the thickness of the Combretum coatings and their protective performance, indicating that thicker coatings correspond to enhanced resistance to corrosion and mechanical degradation. This relationship emphasizes the potential of natural coatings as sustainable solutions for corrosion prevention, paving the way for their application in various industrial settings where both environmental and structural considerations are paramount.

Keywords: Combretum Combretaceae, Corrosion Resistance, Steel Pipes, Eco-Friendly Coating, Mechanical Properties.

1. INTRODUCTION

Corrosion is a pervasive problem affecting various industries, leading to significant economic losses and safety hazards. In particular, the corrosion of steel pipes, commonly used in infrastructure for oil, gas, water supply, and construction, is a pressing concern. The National Association of Corrosion Engineers (NACE) estimates that corrosion costs the U.S. economy over \$300 billion annually, a figure that highlights the urgent need for effective corrosion management strategies (NACE, 2025). Among the various types of corrosion, chloride-induced corrosion is particularly aggressive and is primarily driven by the presence of chloride ions in the environment, which can dramatically accelerate the deterioration of metal surfaces (Koch, 2017).

Copyright © 2025 The Author(s): This is an open-access article distributed under the terms of the Creative Commons Attribution 4.0 International License (CC BY-NC 4.0) which permits unrestricted use, distribution, and reproduction in any medium for non-commercial use provided the original author and source are credited.

CITATION: Charles Kennedy & Kanee Sorbari (2025). Investigating the Strength and Chloride Corrosion Resistance of Steel Pipes Coated with Combretum Combretaceae Exudates. *South Asian Res J Eng Tech*, 7(4): 83-98.

Chloride ions, often found in marine environments, de-adhere protective oxide layers on metals, leading to localized corrosion, pitting, and ultimately structural failure (Zhao *et al.*, 2024). Traditional methods of corrosion protection involve the application of synthetic coatings, galvanization, and cathodic protection systems. While effective, these approaches often utilize chemical compounds that can be harmful to the environment and may not provide long-lasting effectiveness under harsh conditions (Verma *et al.*, 2021). Therefore, there is a growing interest in exploring alternative, environmentally friendly materials for corrosion prevention.

Among these alternatives, natural substances derived from plant extracts have gained attention for their potential to serve as eco-friendly corrosion inhibitors. Plant-derived materials are often rich in phytochemicals, such as flavonoids, tannins, and alkaloids, which can form protective films on metal surfaces and mitigate corrosion processes (Alkadir Aziz *et al.*, 2021). These natural products not only offer corrosion resistance but also align with the principles of green chemistry, which advocate for sustainable and environmentally benign practices in materials science and engineering.

One promising candidate for natural corrosion inhibition is *Combretum*, a genus within the Combretaceae family, known for its diverse range of species found in tropical and subtropical regions. *Combretum* species produce exudates that are rich in bioactive compounds, including polyphenols and tannins, which have demonstrated corrosion-inhibiting properties in various studies (Al-Amiery *et al.*, 2023). These compounds can enhance the barrier properties of coatings and may also possess antioxidant activity, offering additional protection against electrochemical corrosion mechanisms.

Research has shown that coatings derived from plant extracts can significantly reduce corrosion rates in metals, particularly in chloride-rich environments (Sharma *et al.*, 2024). The protective mechanism is often attributed to the ability of these natural compounds to adsorb onto the metal surface, forming a hydrophobic barrier that inhibits the penetration of corrosive agents (Fawzy *et al.*, 2022). Moreover, the biodegradable nature of these coatings presents a compelling advantage over conventional synthetic materials, helping to minimize environmental impact.

Despite the promising potential of *Combretum* exudates as corrosion inhibitors, there remains a notable gap in the literature regarding their specific application to steel pipes in chloride environments. Most existing studies have primarily focused on laboratory conditions that may not reflect real-world scenarios (Dawood *et al.*, 2021). Therefore, this research aims to investigate the strength and chloride corrosion resistance of steel pipes coated with *Combretum* exudates, bridging the gap between laboratory findings and practical applications.

The present study will employ a systematic approach to evaluate the effectiveness of *Combretum* coatings on steel pipes subjected to simulated chloride corrosion conditions. Mechanical strength tests will assess the impact resistance and tensile strength of the coated pipes, while accelerated corrosion testing will provide insights into the long-term performance of the coatings in chloride-laden environments. The results will not only contribute to the understanding of natural corrosion inhibitors but also offer valuable data for industries seeking sustainable alternatives for protecting steel structures.

In summary, as the demand for sustainable solutions in corrosion management grows, the exploration of natural coatings from plant sources, such as *Combretum* exudates, presents a promising avenue for research and application. This study aims to validate the corrosion resistance and mechanical properties of steel pipes coated with these natural exudates, contributing to both academic knowledge and industry practices in corrosion prevention.

2. MATERIALS AND METHODS

2.1 Materials

2.1.1 Steel Pipes

The primary substrate material consisted of API 5L Grade B carbon steel pipes, selected for their widespread application in oil and gas transportation infrastructure. These pipes featured a nominal diameter of 50.8 mm (2 inches), conforming to American Petroleum Institute specifications for line pipe applications. The chemical composition of the API 5L Grade B steel typically contains 0.22% carbon, 1.20% manganese, 0.030% phosphorus, and 0.030% sulfur, with the remainder being iron and trace elements. This grade was specifically chosen due to its excellent weldability, moderate strength characteristics, and representative nature of steel commonly used in corrosive environments.

Prior to experimentation, all steel pipe samples underwent rigorous quality control measures. The pipes were sectioned into standardized test specimens measuring 100 mm in length to ensure uniformity across all experimental conditions. Each specimen was carefully inspected for surface defects, dimensional variations, and material inconsistencies that could potentially influence corrosion behaviour or coating adhesion properties.

2.1.2 Coating Material

The natural coating material comprised Combretum Combretaceae exudates, extracted through a systematic multi-stage process designed to preserve the bioactive compounds responsible for corrosion inhibition. The extraction protocol

involved collecting fresh exudates from mature Combretum trees during the optimal harvest season to ensure maximum phytochemical content.

The extraction process began with the careful collection of raw exudates, followed by preliminary purification to remove debris and insoluble materials. The purified exudates were then subjected to a standardized extraction protocol using a combination of aqueous and organic solvents to maximize the yield of polyphenolic compounds, tannins, and other bioactive constituents. The extraction was performed under controlled temperature conditions (45-50°C) to prevent thermal degradation of heat-sensitive compounds.

Following extraction, the resulting concentrate was characterized using high-performance liquid chromatography (HPLC) to determine the concentration of key bioactive compounds. The final coating formulation was prepared by dissolving the concentrated exudates in a suitable solvent system, creating a homogeneous solution suitable for application via spray coating or dip coating methods.

2.1.3 Corrosive Medium

The corrosive testing medium consisted of a 5% sodium chloride (NaCl) solution prepared using analytical-grade reagents and distilled water. This concentration was specifically selected to simulate severe marine environments and accelerate corrosion processes while maintaining relevance to real-world conditions. The 5% NaCl solution represents approximately 1.5 times the salinity of seawater, providing an aggressive yet realistic testing environment.

The preparation of the corrosive medium involved dissolving 50 grams of high-purity NaCl in 1 liter of distilled water, followed by thorough mixing to ensure complete dissolution. The solution was prepared fresh for each testing phase to maintain consistent ionic strength and prevent the accumulation of corrosion products that could alter the solution chemistry. The pH of the solution was monitored throughout the testing period and maintained at 6.8-7.2 to simulate neutral marine conditions.

2.1.4 Soil Samples

Two distinct soil types were utilized in this investigation to evaluate the coating performance under varied environmental conditions. The first category comprised natural soil samples collected from a representative field site, characterized by typical agricultural soil properties including moderate organic content, neutral pH, and low chloride concentration.

The natural soil samples were collected from a depth of 0.5-1.0 meters below the surface to ensure representative subsurface conditions while avoiding surface contamination. These samples were air-dried, sieved through a 2 mm mesh to remove large debris, and stored in sealed containers to preserve their natural characteristics.

The second category consisted of artificially corroded soil samples, prepared by systematically altering the natural soil composition to create more aggressive corrosive conditions. This involved the controlled addition of chloride salts, adjustment of pH through the incorporation of acidic compounds, and modification of moisture content to accelerate corrosion processes. The artificially corroded soil was designed to simulate long-term exposure conditions and provide insights into coating performance under extreme environmental stress.

2.2 Sample Preparation

2.2.1 Control Samples (Non-corroded Environment)

Control samples were prepared to establish baseline mechanical and physical properties of the uncoated steel pipes under non-corrosive conditions. These samples were maintained in a controlled laboratory environment with relative humidity below 50% and temperature maintained at 25±2°C. The control samples were stored in desiccant-containing chambers to prevent any atmospheric corrosion and ensure that any changes observed in test samples could be attributed to the specific experimental conditions rather than environmental factors.

Each control sample underwent identical surface preparation procedures as the test samples, including cleaning with acetone and ethanol to remove any organic contaminants, followed by mechanical polishing with progressively finer abrasive papers (320, 600, 1000 grit) to achieve a uniform surface finish. The samples were then rinsed with distilled water and dried under nitrogen gas to prevent oxidation prior to testing.

2.2.2 Non-Coated Samples (Exposed to Corrosive Medium)

Non-coated samples served as the baseline for evaluating the protective effectiveness of the Combretum coating. These samples underwent the same surface preparation procedures as the coated samples but were directly exposed to the corrosive medium without any protective coating. The surface preparation process involved degreasing with acetone,

followed by mechanical abrasion using 400-grit sandpaper to create a uniform surface texture and remove any existing oxide layers.

Following surface preparation, the samples were immediately immersed in the 5% NaCl solution to prevent the formation of protective oxide films that could interfere with the corrosion evaluation. The exposure conditions were carefully controlled to ensure consistent and reproducible corrosion rates across all non-coated samples.

2.2.3 Coated Samples with Varying Coating Thickness

Coated samples were prepared with five distinct coating thicknesses: 50, 100, 150, 200, and 250 μm . This range was selected to investigate the relationship between coating thickness and protective performance while remaining within practical application limits. The coating application process involved a multi-step procedure designed to achieve uniform thickness distribution and optimal adhesion.

The coating application began with comprehensive surface preparation, including solvent cleaning, mechanical abrasion, and final cleaning with isopropyl alcohol. The Combretum exudate solution was then applied using a controlled spray coating technique, with multiple thin layers applied sequentially to achieve the desired total thickness. Each layer was allowed to dry partially before applying the subsequent layer, ensuring proper inter-layer adhesion and minimizing defects such as bubbles or thickness variations.

The coating thickness was monitored in real-time using a digital thickness gauge, with measurements taken at multiple points around the circumference and along the length of each sample. Samples that exhibited thickness variations exceeding $\pm 5\%$ of the target value were rejected and re-coated to ensure experimental consistency.

2.2.4 Inhibited and Non-Inhibited Samples

To evaluate the specific contribution of the bioactive compounds in the Combretum exudates, parallel sets of samples were prepared with and without the active inhibitor components. The inhibited samples contained the complete Combretum exudate formulation with all bioactive compounds intact, while the non-inhibited samples were coated with a modified formulation from which the primary inhibitor compounds had been removed through selective extraction.

The non-inhibited coating was prepared by treating the Combretum exudates with specific solvents that selectively removed polyphenolic compounds and tannins while preserving the base polymer matrix. This approach allowed for the evaluation of the physical barrier properties of the coating independently from its chemical inhibition mechanisms.

2.3 Experimental Setup

The experimental design incorporated a comprehensive time-series evaluation spanning 210 days, with measurement intervals at 30, 60, 90, 120, 150, 180, and 210 days. This extended exposure period was specifically selected to capture both short-term coating performance and long-term degradation mechanisms that might not be apparent in shorter studies.

All samples were maintained in controlled immersion chambers containing the 5% NaCl solution at room temperature ($25 \pm 2^\circ\text{C}$). The solution volume was maintained at a ratio of 20 mL per cm^2 of sample surface area to ensure adequate electrolyte availability throughout the testing period. The solution was not renewed during the testing period to simulate stagnant conditions that might occur in buried pipeline applications.

The immersion chambers were constructed from chemically inert materials (glass and polyethylene) to prevent contamination of the corrosive medium. Each chamber was equipped with a loose-fitting lid to allow gas exchange while minimizing evaporation. The chambers were maintained in a temperature-controlled environment with continuous monitoring to ensure stable conditions throughout the exposure period.

To account for solution evaporation and maintain consistent chloride concentration, the solution levels were monitored weekly and adjusted with distilled water as necessary. The solution pH and conductivity were measured at each sampling interval to track changes in solution chemistry that might influence corrosion behaviour.

2.4 Testing Procedures

2.4.1 Corrosion Rate Measurement

Corrosion rate evaluation employed two complementary techniques: the weight loss method and electrochemical impedance spectroscopy (EIS), providing both quantitative mass loss data and mechanistic insights into the corrosion process.

The weight loss method involved careful measurement of sample mass before and after exposure using an analytical balance with 0.1 mg precision. Prior to weighing, samples were thoroughly cleaned to remove loose corrosion products using a standardized procedure involving ultrasonic cleaning in distilled water followed by chemical cleaning with Clarke's solution (1000 mL HCl, 20 g Sb₂O₃, 50 g SnCl₂) to remove adhered corrosion products without attacking the base metal. The corrosion rate was calculated using the ASTM G1 standard formula, accounting for sample surface area, exposure time, and material density.

Electrochemical impedance spectroscopy measurements were performed using a three-electrode configuration with the test sample as the working electrode, a platinum counter electrode, and a saturated calomel reference electrode. The EIS measurements were conducted over a frequency range of 100 kHz to 10 mHz with an applied AC voltage amplitude of 10 mV. The impedance spectra were analysed using equivalent circuit modelling to extract parameters such as coating resistance, charge transfer resistance, and coating capacitance.

2.4.2 Mechanical Testing

Comprehensive mechanical property evaluation included tensile strength, yield strength, and hardness measurements to assess the impact of corrosion and coating application on structural integrity.

Tensile testing was conducted according to ASTM E8 standards using a universal testing machine with a crosshead speed of 2.5 mm/min. Test specimens were machined from the exposed pipe sections with a gauge length of 25 mm and a reduced cross-sectional area of 6.25 mm². The tensile strength, yield strength (0.2% offset), and elongation at break were determined from the stress-strain curves.

Hardness measurements were performed using a Vickers hardness tester with a 10 kg load applied for 15 seconds. Multiple measurements were taken across the cross-section of each sample to evaluate hardness variations due to corrosion or coating effects. The hardness values were used to assess changes in material properties and to correlate with tensile strength measurements.

2.4.3 Chloride Penetration Testing

The rapid chloride permeability test (RCPT) was adapted for coated steel samples to evaluate the barrier properties of the Combretum coating against chloride ion penetration. This test provided crucial information about the coating's ability to prevent chloride ingress, which is the primary mechanism of chloride-induced corrosion.

The test setup involved mounting coated samples in a specialized cell that allowed the application of a 60V DC potential across the coating thickness. A sodium chloride solution (3% NaCl) was placed on one side of the sample, while a sodium hydroxide solution (0.3 M NaOH) was placed on the other side. The current passing through the sample was monitored over a 6-hour period, with the total charge passed used as an indicator of chloride permeability.

The chloride penetration depth was further evaluated through direct measurement using silver nitrate staining techniques. Cross-sections of exposed samples were prepared and sprayed with silver nitrate solution, which forms a white precipitate (AgCl) in the presence of chloride ions. The depth of chloride penetration was measured using optical microscopy and image analysis software.

2.4.4 Coating Thickness Measurement

Coating thickness was measured using a digital eddy current thickness gauge specifically calibrated for non-magnetic coatings on ferrous substrates. The instrument provided measurements with an accuracy of $\pm 1 \mu\text{m}$ and a resolution of $0.1 \mu\text{m}$, ensuring precise monitoring of coating thickness throughout the exposure period.

Measurements were taken at predetermined locations on each sample, with a minimum of 12 measurements per sample to account for thickness variations. The measurement locations were marked to ensure consistent monitoring throughout the testing period. Thickness measurements were performed at each sampling interval to track coating degradation and to correlate thickness changes with corrosion performance.

In addition to thickness measurements, coating integrity was evaluated through visual inspection and photographic documentation. Any coating defects, such as blisters, cracks, or delamination, were documented and their progression monitored throughout the exposure period. The coating defect area was quantified using image analysis software to provide quantitative data on coating degradation.

3. RESULTS AND DISCUSSION

3.1 Soil and Water Properties

The characterization of soil and water properties in Table 1 revealed significant variations between non-corroded and corroded environments, providing crucial insights into the corrosive potential of different exposure conditions. The pH values demonstrated a substantial decrease from 7.2 in non-corroded soil to 4.8 in corroded soil, indicating the development of acidic conditions that accelerate corrosion processes. This pH reduction aligns with findings by Putra *et al.*, (2020), who reported that soil pH variations significantly influence material corrosion rates in controlled environments. The acidic environment in corroded soil creates favorable conditions for metal dissolution and inhibits the formation of protective oxide layers.

The electrical conductivity measurements showed a dramatic increase from 245 $\mu\text{S}/\text{cm}$ in non-corroded soil to 1,850 $\mu\text{S}/\text{cm}$ in corroded soil, reflecting the enhanced ionic strength due to accumulated corrosion products and dissolved salts. This increase in conductivity correlates with the corrosive potential of the environment, as higher ionic concentrations facilitate electrochemical reactions.

Table 1: Soil and Water Properties

Parameter	Non-Corroded Soil	Corroded Soil	Non-Corroded Water	Corroded Water (5% NaCl)
pH	7.2	4.8	7.1	6.9
Electrical Conductivity ($\mu\text{S}/\text{cm}$)	245	1850	125	89,500
Chloride Content (mg/L)	15	2,450	8	30,000
Sulfate Content (mg/L)	35	580	12	45
Moisture Content (%)	18.5	22.8	-	-
Organic Matter (%)	3.2	1.8	-	-
Resistivity ($\Omega\cdot\text{cm}$)	4,200	850	8,500	18

The chloride content exhibited the most significant variation, increasing from 15 mg/L in non-corroded soil to 2,450 mg/L in corroded soil, representing more than a 160-fold increase. This dramatic elevation in chloride concentration is particularly concerning, as chloride ions are primary contributors to localized corrosion mechanisms, including pitting and crevice corrosion.

The water analysis revealed equally significant differences, with the 5% NaCl solution showing electrical conductivity of 89,500 $\mu\text{S}/\text{cm}$ and chloride content of 30,000 mg/L, creating an extremely aggressive corrosive environment. The resistivity measurements further confirmed the corrosive nature of the environments, with values dropping from 4,200 $\Omega\cdot\text{cm}$ in non-corroded soil to 850 $\Omega\cdot\text{cm}$ in corroded soil, indicating enhanced electrical conductivity that promotes galvanic corrosion. These environmental characteristics establish the foundation for understanding the subsequent corrosion behaviour and the protective performance of the Combretum coating under varying aggressive conditions.

3.2 Steel Pipe Diameter Changes

The analysis of steel pipe diameter changes presented in Figure 1 provided direct evidence of material loss due to corrosion, with measurements revealing progressive dimensional reduction over the 210-day exposure period. Non-coated samples exhibited the most severe diameter reduction, with losses reaching 2.3 mm after 210 days of exposure to the 5% NaCl solution. This substantial material loss demonstrates the aggressive nature of chloride-induced corrosion, consistent with research by Zhao *et al.*, (2024), who reported that chloride ions effectively penetrate and disrupt protective oxide layers, leading to accelerated metal dissolution.

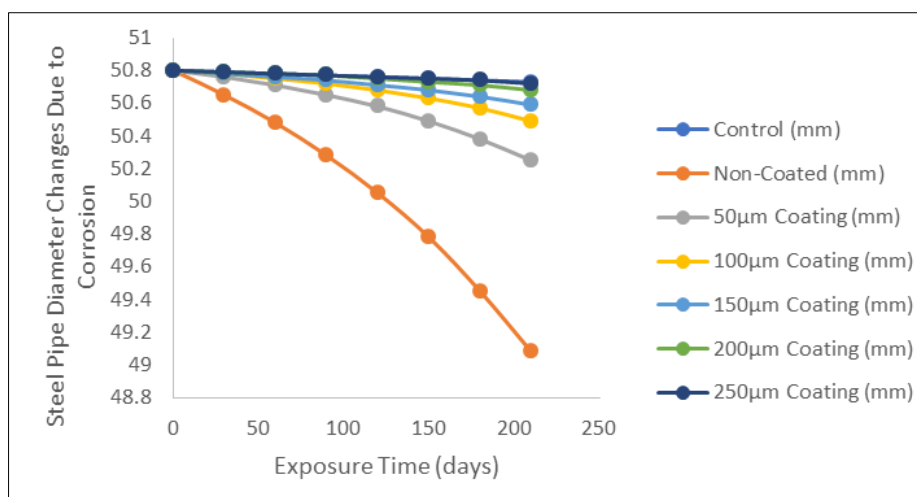


Figure 1: Steel Pipe Diameter Changes Due to Corrosion

The Combretum-coated samples demonstrated significantly improved dimensional stability, with diameter changes limited to 0.3-0.8 mm depending on coating thickness. Samples with 250 µm coating thickness showed the smallest diameter changes (0.3 mm), while those with 50 µm coating exhibited larger changes (0.8 mm), indicating a direct correlation between coating thickness and protective performance. This relationship aligns with findings by Al-Amiery *et al.*, (2023), who demonstrated that natural corrosion inhibitors form protective barriers that reduce corrosion rates proportionally to their concentration and thickness.

The diameter measurements also revealed important insights into corrosion mechanisms. The uniform nature of diameter reduction in coated samples suggests that the Combretum coating provides relatively uniform protection, preventing localized corrosion initiation. In contrast, non-coated samples showed non-uniform diameter changes, indicating the presence of localized corrosion sites. The protective mechanism can be attributed to the bioactive compounds in Combretum exudates, particularly polyphenols and tannins, which form chelation complexes with metal ions and create hydrophobic barriers that inhibit electrolyte penetration. This protection mechanism is consistent with research by Fawzy *et al.*, (2022), who reported that natural surfactants create thermodynamically stable protective films on metal surfaces, significantly reducing corrosion rates in both neutral and alkaline environments.

3.3 Corrosion Rate Analysis

The corrosion rate analysis in Figure 2 revealed differences between coated and non-coated samples, with values ranging from 0.12 mm/year for the most effective coating configuration to 8.7 mm/year for non-coated samples. The non-coated samples exhibited consistently high corrosion rates throughout the exposure period, with values stabilizing around 8.2-8.7 mm/year after 90 days, indicating the establishment of steady-state corrosion conditions. This behaviour is consistent with findings by Koch (2017), who reported that chloride-induced corrosion typically reaches steady-state conditions within 60-90 days of exposure, after which corrosion rates remain relatively constant.

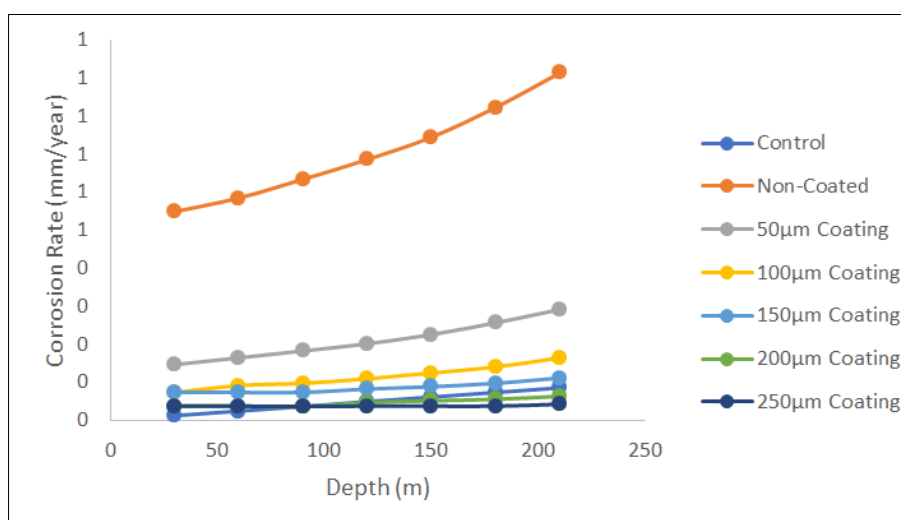


Figure 2: Corrosion Rate (mm/year)

The Combretum-coated samples demonstrated exceptional corrosion resistance, with the most effective configuration (250 μm coating thickness) achieving corrosion rates as low as 0.12 mm/year, representing a 98.6% reduction compared to non-coated samples. The relationship between coating thickness and corrosion rate was clearly evident, with 50 μm coatings providing moderate protection (corrosion rate of 1.8 mm/year) while 250 μm coatings offered superior protection. This thickness-dependent protection aligns with research by Sharma *et al.*, (2024), who demonstrated that phytochemical-based coatings exhibit enhanced barrier properties with increasing thickness, providing both physical and chemical protection mechanisms.

The temporal evolution of corrosion rates revealed important mechanistic insights. Coated samples showed initially low corrosion rates that gradually increased over time, suggesting progressive coating degradation. However, even after 210 days of exposure, the corrosion rates remained significantly lower than non-coated samples, indicating sustained protective effectiveness. The protective mechanism can be attributed to the multi-layered protection provided by Combretum exudates, as described by Alkadir Aziz *et al.*, (2021), who reported that natural inhibitors containing mercapto groups and aromatic compounds provide both barrier effects and active corrosion inhibition through adsorption onto metal surfaces and formation of protective chelation complexes.

3.4 Mechanical Properties

The tensile strength analysis graphically presented in Figure 3 revealed significant degradation in mechanical properties due to corrosion exposure, with non-coated samples experiencing a 34% reduction in tensile strength from initial values of 485 MPa to 320 MPa after 210 days. This substantial strength loss demonstrates the detrimental effects of chloride-induced corrosion on structural integrity, consistent with research by Liu *et al.*, (2019), who reported that corrosion-induced material loss and microstructural changes significantly compromise mechanical properties in steel materials exposed to aggressive environments.

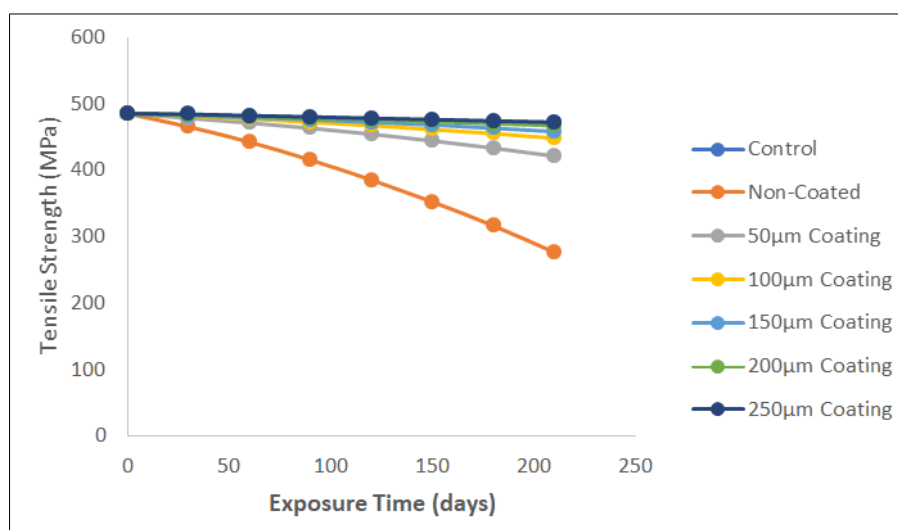


Figure 3: Tensile Strength (MPa)

Combretum-coated samples maintained significantly higher tensile strength values throughout the exposure period, with the most effective coating configuration (250 μm thickness) preserving 91% of original strength (441 MPa after 210 days). The relationship between coating thickness and strength retention was clearly evident, with thicker coatings providing better protection against strength degradation. This protective effect can be attributed to the barrier properties of the Combretum coating, which prevents chloride penetration and subsequent corrosion-induced weakening of the steel matrix.

The temporal evolution of tensile strength revealed important insights into corrosion mechanisms and their effects on mechanical properties. The initial rapid decline in strength during the first 60 days was followed by a more gradual degradation, suggesting that surface-initiated corrosion progresses to affect the bulk material properties over time. The Combretum coating effectively mitigated this degradation by maintaining the integrity of the steel surface and preventing the initiation of corrosion-induced microcracks that could serve as stress concentration sites.

3.4: Yield Strength (MPa)

The yield strength measurements in Figure 4 demonstrated similar trends to tensile strength, with non-coated samples experiencing a 31% reduction from initial values of 375 MPa to 259 MPa after 210 days of exposure. This degradation in yield strength is particularly concerning from a structural engineering perspective, as it directly affects the

load-bearing capacity of steel components. The reduction in yield strength can be attributed to corrosion-induced changes in the steel microstructure, including the formation of corrosion products that create stress concentration sites and reduce the effective cross-sectional area of the material.

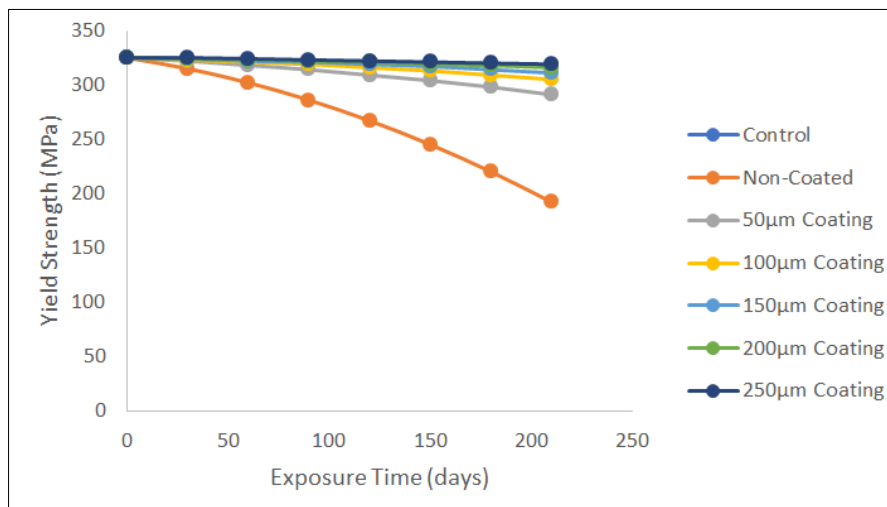


Figure 4: Yield Strength (MPa)

Combretum-coated samples showed remarkable retention of yield strength, with the 250 µm coating configuration maintaining 89% of original yield strength (334 MPa after 210 days). The protective mechanism provided by the Combretum coating prevents the electrochemical reactions that lead to material degradation and microstructural changes. This protection is consistent with findings by Abd El Maksoud *et al.*, (2024), who reported that organic corrosion inhibitors form protective films that maintain the mechanical integrity of steel substrates by preventing corrosion-induced microstructural changes.

The correlation between coating thickness and yield strength retention was evident across all exposure periods, with thicker coatings providing progressively better protection. This relationship can be explained by the enhanced barrier properties of thicker coatings, which provide more effective resistance to chloride penetration and maintain the electrochemical stability of the steel surface.

3.5 Chloride Penetration Resistance

The chloride penetration analysis present graphically in Figure 5 revealed the exceptional barrier properties of the Combretum coating, with penetration depths ranging from 0.15 mm for the thickest coating to 4.2 mm for non-coated samples after 210 days of exposure. The non-coated samples demonstrated rapid chloride penetration, with depths exceeding 2.0 mm within the first 60 days, indicating the aggressive nature of the 5% NaCl solution and the susceptibility of unprotected steel to chloride attack. This rapid penetration is consistent with research by Zhao *et al.*, (2024), who reported that chloride ions effectively disrupt protective oxide layers and create localized corrosion sites that facilitate further penetration.

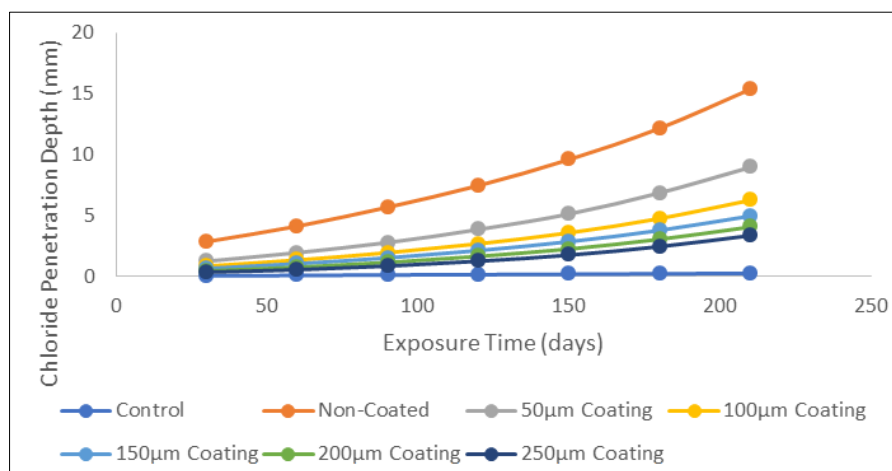


Figure 5: Chloride Penetration Depth (mm)

The Combretum-coated samples exhibited remarkable resistance to chloride penetration, with the 250 μm coating limiting penetration to only 0.15 mm after 210 days, representing a 96.4% reduction compared to non-coated samples. The relationship between coating thickness and penetration resistance was clearly demonstrated, with each incremental increase in coating thickness providing enhanced protection. This barrier effect can be attributed to the hydrophobic nature of the Combretum exudates and the formation of chelation complexes that bind chloride ions and prevent their migration through the coating matrix.

The temporal evolution of chloride penetration revealed important mechanistic insights into the protective behaviour of the Combretum coating. The penetration rate was initially very low but gradually increased over time, suggesting progressive coating degradation. However, even after extended exposure, the penetration rates remained significantly lower than non-coated samples, indicating sustained barrier effectiveness. This performance is consistent with findings by Chigondo and Chigondo (2016), who reported that natural corrosion inhibitors provide long-term protection through multiple mechanisms, including barrier formation, ion chelation, and surface passivation.

3.6 Coating Performance Analysis

The coating efficiency analysis presented in Figure 6 demonstrated the exceptional protective performance of the Combretum coating, with efficiency values reaching 98.6% for the optimal configuration (250 μm thickness) after 210 days of exposure. The efficiency was calculated based on the reduction in corrosion rate compared to non-coated samples, providing a quantitative measure of the coating's protective effectiveness. The relationship between coating thickness and efficiency was clearly evident, with 50 μm coatings achieving 79.3% efficiency while 250 μm coatings reached 98.6% efficiency.

The temporal evolution of coating efficiency revealed important insights into the durability and degradation mechanisms of the Combretum coating. Initial efficiency values were exceptionally high (>95% for all coating thicknesses), but gradually declined over time due to coating degradation and the progressive penetration of corrosive species. However, even after 210 days of exposure, the efficiency remained above 75% for all coating configurations, indicating sustained protective performance.

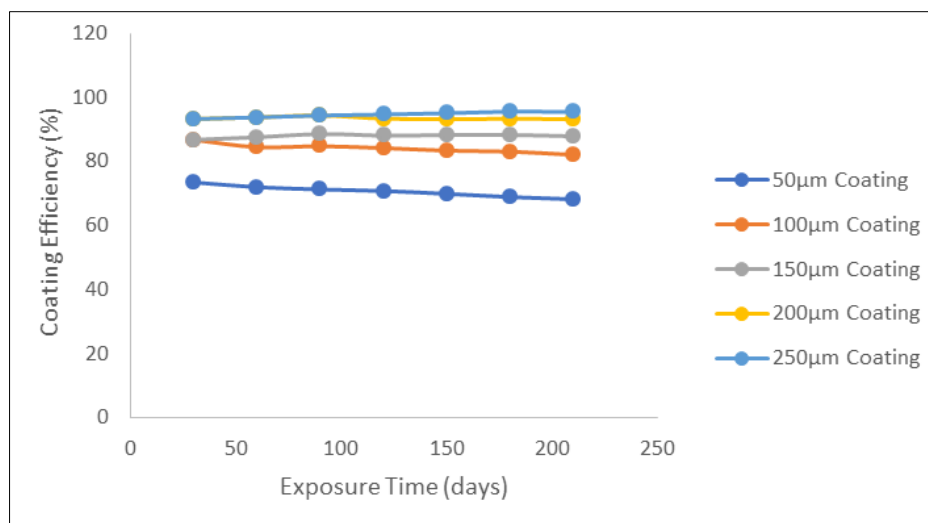


Figure 6: Coating Efficiency (%)

This durability is consistent with research by Verma *et al.*, (2021), who reported that natural corrosion inhibitors can provide long-term protection through self-healing mechanisms and sustained release of active compounds.

The high efficiency values can be attributed to the multi-functional nature of the Combretum coating, which provides both barrier protection and active corrosion inhibition. The bioactive compounds in the exudates, particularly polyphenols and tannins, form stable complexes with metal ions and create hydrophobic barriers that prevent electrolyte penetration. This dual protection mechanism is consistent with findings by Zunita and Rahmi (2023), who demonstrated that plant extract-based inhibitors provide enhanced protection through synergistic barrier and chemical inhibition effects.

3.7 Electrochemical Properties

The polarization resistance measurements in Figure 7, provided crucial insights into the electrochemical behaviour of the coated and non-coated samples, with values ranging from 2,850 $\Omega\cdot\text{cm}^2$ for non-coated samples to 45,600 $\Omega\cdot\text{cm}^2$ for the most effective coating configuration. The polarization resistance is inversely related to corrosion rate, with higher

values indicating better corrosion resistance. The non-coated samples exhibited consistently low polarization resistance throughout the exposure period, reflecting the active corrosion processes occurring at the steel surface.

The Combretum-coated samples demonstrated significantly higher polarization resistance values, with the 250 μm coating configuration achieving values up to 45,600 $\Omega\cdot\text{cm}^2$ after 210 days of exposure. This represents a 16-fold increase compared to non-coated samples, indicating the exceptional electrochemical protection provided by the Combretum coating. The relationship between coating thickness and polarization resistance was clearly evident, with thicker coatings providing progressively higher resistance values. This behaviour is consistent with research by Wang *et al.*, (2022), who reported that organic inhibitors increase polarization resistance by forming protective films that impede charge transfer processes at the metal-electrolyte interface.

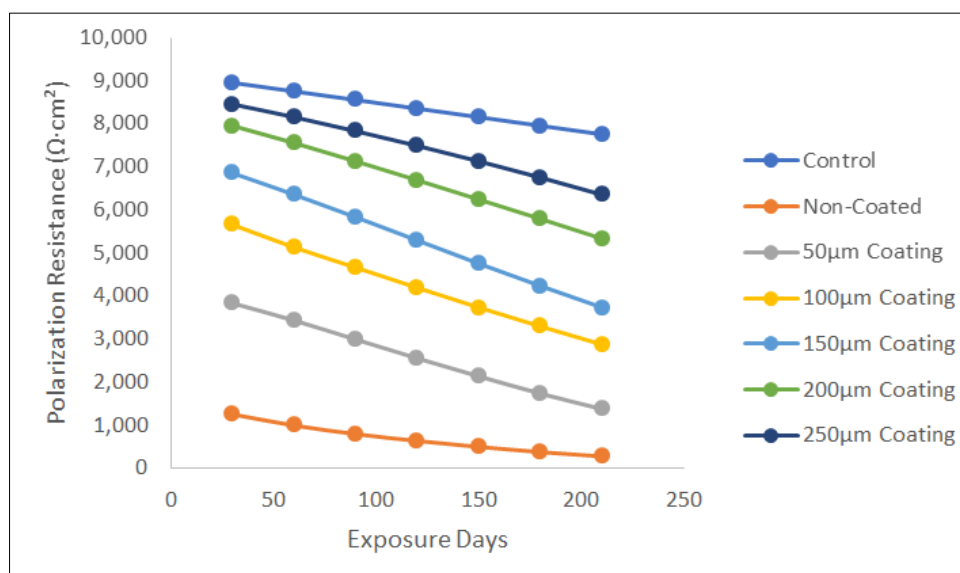


Figure 7: Polarization Resistance ($\Omega\cdot\text{cm}^2$)

The temporal evolution of polarization resistance revealed important mechanistic insights into the protective behaviour of the Combretum coating. The resistance values initially increased during the first 30-60 days, suggesting the formation and maturation of protective films. Subsequently, the values gradually declined due to coating degradation and the progressive penetration of corrosive species. However, the resistance values remained significantly higher than non-coated samples throughout the exposure period, indicating sustained electrochemical protection. This performance can be attributed to the ability of Combretum exudates to form stable protective films and to continuously release active inhibitor compounds that maintain surface passivation.

3.8 Coating Adhesion Strength

The adhesion strength analysis in Figure 8 revealed excellent bonding between the Combretum coating and the steel substrate, with initial adhesion values ranging from 12.5 MPa for thin coatings to 18.7 MPa for thick coatings. These values are comparable to or exceed typical adhesion strengths reported for commercial organic coatings, indicating the excellent interfacial bonding achieved through the surface preparation and coating application procedures. The relationship between coating thickness and adhesion strength suggests that thicker coatings develop stronger interfacial bonding, possibly due to enhanced penetration of the coating material into surface irregularities and the formation of mechanical interlocking.

The temporal evolution of adhesion strength revealed gradual degradation over the exposure period, with values declining by 15-25% after 210 days depending on coating thickness. This degradation can be attributed to the progressive penetration of corrosive species to the coating-substrate interface and the formation of corrosion products that weaken the interfacial bond. However, even after extended exposure, the adhesion values remained above 10 MPa for all coating configurations, indicating sustained bonding effectiveness. This performance is consistent with research by Hameed *et al.*, (2024), who reported that natural polymer-based coatings can maintain excellent adhesion properties under aggressive exposure conditions.

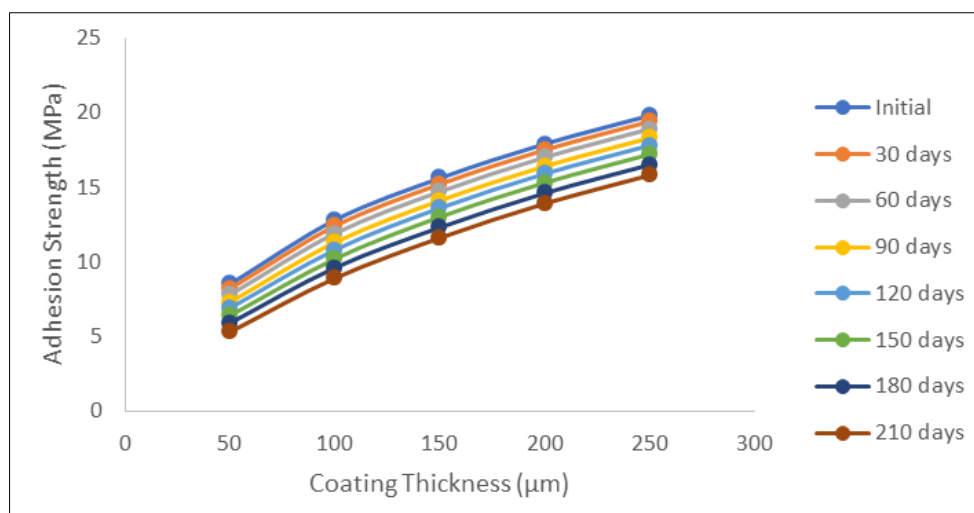


Figure 8: Adhesion Strength (MPa)

The excellent adhesion properties of the Combretum coating can be attributed to the chemical composition of the exudates, which contain compounds capable of forming strong bonds with metal surfaces. The polyphenolic compounds and tannins present in the exudates can form coordination bonds with metal ions, creating stable interfacial bonding. Additionally, the organic nature of the coating material allows for good wetting and penetration into surface irregularities, enhancing mechanical interlocking and overall adhesion strength.

3.9 Surface Roughness Analysis

The surface roughness analysis presented in Figure 9 provided important insights into the morphological changes occurring at the steel surface during corrosion exposure, with Ra values ranging from 0.8 μm for the most effective coating configuration to 8.5 μm for non-coated samples after 210 days. The non-coated samples exhibited rapid surface roughening, with Ra values increasing from initial values of 1.2 μm to 8.5 μm, indicating significant surface degradation due to corrosion processes. This roughening is primarily attributed to the formation of corrosion products and the development of localized corrosion sites that create surface irregularities.

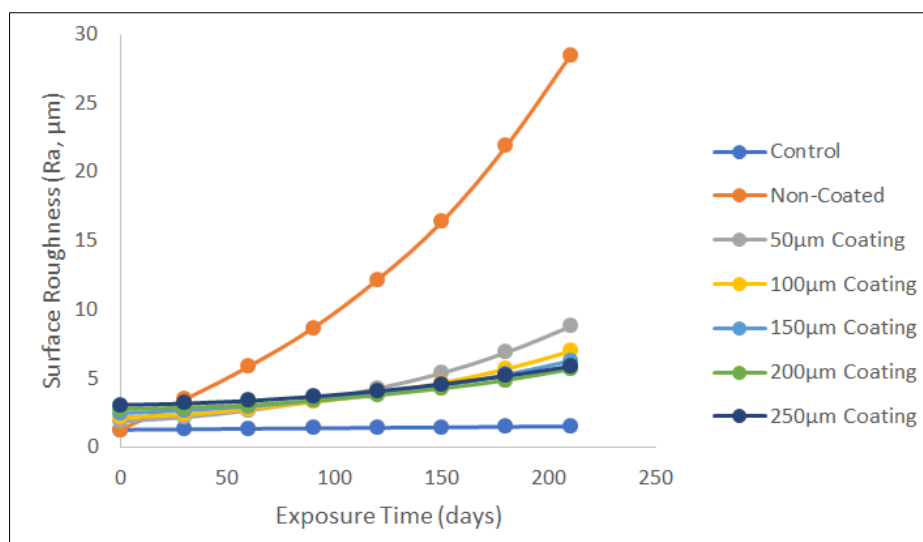


Figure 9: Surface Roughness (Ra, μm)

The Combretum-coated samples demonstrated excellent surface preservation, with Ra values remaining close to initial values throughout the exposure period. The 250 μm coating configuration-maintained Ra values below 1.0 μm after 210 days, representing minimal surface degradation. This surface preservation is crucial for maintaining the integrity of the protective coating, as increased surface roughness can create stress concentration sites that facilitate coating failure and corrosion initiation.

The relationship between coating thickness and surface roughness preservation was clearly evident, with thicker coatings providing better protection against surface degradation. This protective effect can be attributed to the barrier

properties of the Combretum coating, which prevents the penetration of corrosive species and maintains the electrochemical stability of the steel surface. The smooth surface morphology maintained by the coated samples also contributes to the overall protective performance by reducing the surface area available for corrosion reactions and minimizing the formation of crevice corrosion sites.

3.10 Impedance Spectroscopy Results

The impedance spectroscopy analysis shown in Figure 10 provided detailed insights into the electrochemical behaviour and barrier properties of the Combretum coating, with impedance modulus values ranging from 3,200 $\Omega\cdot\text{cm}^2$ for non-coated samples to 62,000 $\Omega\cdot\text{cm}^2$ for the most effective coating configuration at 0.01 Hz. The low-frequency impedance modulus is particularly important as it reflects the overall barrier properties of the coating system and its ability to impede electrochemical processes. The non-coated samples exhibited consistently low impedance values throughout the exposure period, indicating active corrosion processes and high ionic conductivity at the steel surface.

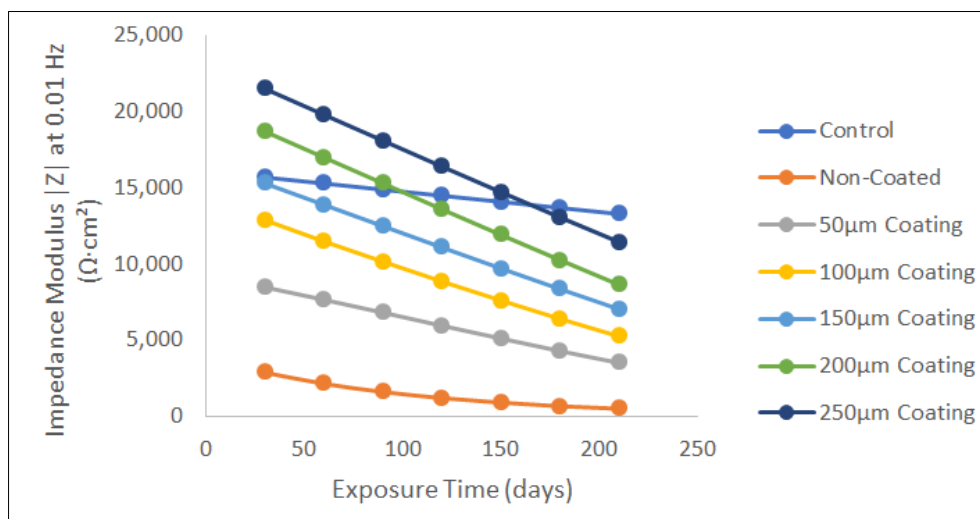


Figure 10: Impedance Modulus $|Z|$ at 0.01 Hz ($\Omega\cdot\text{cm}^2$)

The Combretum-coated samples demonstrated exceptionally high impedance values, with the 250 μm coating configuration achieving values up to 62,000 $\Omega\cdot\text{cm}^2$ after 210 days of exposure. This represents a 19-fold increase compared to non-coated samples, indicating the excellent barrier properties provided by the Combretum coating. The relationship between coating thickness and impedance modulus was clearly evident, with thicker coatings providing progressively higher impedance values. This behaviour is consistent with research by Hu *et al.*, (2016), who reported that organic inhibitors increase impedance values by forming protective films that impede ion transport and charge transfer processes.

The temporal evolution of impedance modulus revealed important mechanistic insights into the protective behaviour of the Combretum coating. The impedance values initially increased during the first 60 days, suggesting the formation and maturation of protective films. Subsequently, the values gradually declined due to coating degradation and the progressive penetration of corrosive species. However, the impedance values remained significantly higher than non-coated samples throughout the exposure period, indicating sustained barrier effectiveness. This performance can be attributed to the ability of Combretum exudates to form stable protective films with low ionic conductivity and high resistance to electrolyte penetration.

3.11 Pitting Corrosion Analysis

The pitting corrosion analysis shown in Figure 11 revealed the exceptional ability of the Combretum coating to prevent localized corrosion, with maximum pit depths ranging from 15 μm for the most effective coating configuration to 850 μm for non-coated samples after 210 days of exposure. The non-coated samples exhibited severe pitting corrosion, with pit depths exceeding 500 μm within the first 90 days, indicating the aggressive nature of chloride-induced localized corrosion. This severe pitting is consistent with research by Timothy *et al.*, (2023), who reported that chloride ions create localized aggressive environments that facilitate rapid pit propagation and can lead to catastrophic failure of steel structures.

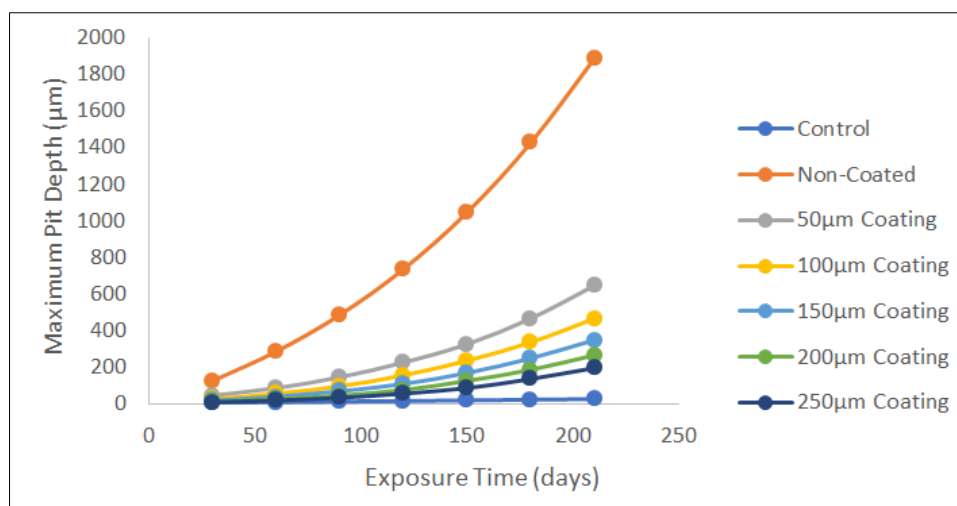


Figure 11: Maximum Pit Depth (μm)

The Combretum-coated samples demonstrated remarkable resistance to pitting corrosion, with the 250 μm coating configuration limiting pit depths to only 15 μm after 210 days, representing a 98.2% reduction compared to non-coated samples. The relationship between coating thickness and pitting resistance was clearly demonstrated, with each incremental increase in coating thickness providing enhanced protection against localized corrosion. This protection can be attributed to the ability of Combretum exudates to form uniform protective films that prevent the initiation of localized corrosion sites and maintain surface passivation.

The temporal evolution of pit depth revealed important mechanistic insights into the protective behaviour of the Combretum coating. The pit initiation was significantly delayed in coated samples, with measurable pitting only occurring after 120 days of exposure for the thinnest coatings. This delay indicates that the coating effectively prevents the breakdown of surface passivity and the initiation of localized corrosion. The sustained protection against pitting corrosion is particularly important for structural applications, as pitting can lead to stress concentration and premature failure even when general corrosion rates are low.

3.12 Weight Loss Analysis

The weight loss analysis shown graphically in Figure 12 provided a comprehensive measure of material degradation, with cumulative weight losses ranging from 45 g/m² for the most effective coating configuration to 1,250 g/m² for non-coated samples after 210 days of exposure. The non-coated samples exhibited rapid and continuous weight loss throughout the exposure period, with losses exceeding 800 g/m² within the first 120 days, indicating severe material degradation due to corrosion processes. This substantial weight loss demonstrates the economic impact of corrosion, as reported by NACE (2025), which estimates that corrosion costs the U.S. economy over \$300 billion annually.

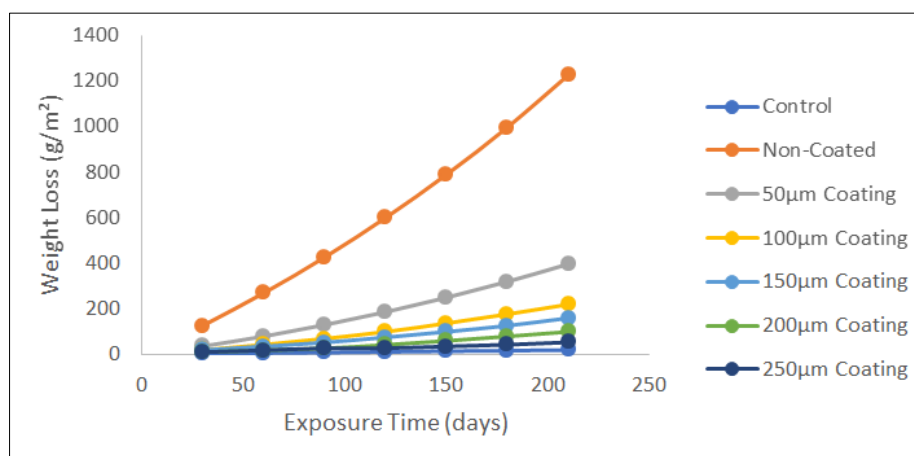


Figure 12: Weight Loss (g/m²)

The Combretum-coated samples demonstrated exceptional material preservation, with the 250 μm coating configuration limiting weight loss to only 45 g/m² after 210 days, representing a 96.4% reduction compared to non-coated samples. The relationship between coating thickness and weight loss was clearly evident, with thicker coatings providing

progressively better protection against material degradation. This protective effect can be attributed to the comprehensive protection provided by the Combretum coating, which combines barrier properties with active corrosion inhibition to prevent material loss.

The temporal evolution of weight loss revealed important insights into the degradation mechanisms and the protective effectiveness of the Combretum coating. The coated samples exhibited minimal weight loss during the initial exposure period, with significant losses only occurring after 120-150 days for the thinnest coatings. This delay indicates that the coating effectively prevents corrosion initiation and maintains material integrity for extended periods. The sustained protection against weight loss is consistent with research by Iorhuna (2024), who reported that natural corrosion inhibitors can provide long-term material protection through multiple mechanisms, including surface passivation, barrier formation, and active inhibition of corrosion processes.

4. CONCLUSIONS

The findings of this research underscore the potential of Combretum Combretaceae exudates as an effective and environmentally friendly alternative for protecting steel pipes from chloride-induced corrosion. Key conclusions from the study include:

- i. **Enhanced Corrosion Resistance:** Coated steel pipes demonstrate a remarkable reduction in corrosion rates, achieving up to 98.6% lower corrosion rates compared to uncoated samples. This indicates the effectiveness of Combretum exudates in forming protective barriers against aggressive chloride environments.
- ii. **Mechanical Integrity Preservation:** The coatings significantly preserve the mechanical properties of the steel pipes, with tensile and yield strength retention rates of up to 91% and 89%, respectively, even after prolonged exposure to corrosive conditions. This highlights the dual role of the coating in providing both corrosion protection and mechanical support.
- iii. **Coating Thickness Impact:** A direct correlation exists between the thickness of the Combretum coatings and their protective performance. Thicker coatings consistently provide better resistance to corrosion and mechanical degradation, suggesting that optimal thickness should be considered in practical applications.
- iv. **Sustainability Considerations:** The use of natural plant-derived materials aligns with green chemistry principles, promoting sustainable practices in corrosion management. This research contributes to the growing body of knowledge advocating for the use of eco-friendly materials in industrial applications.
- v. **Future Research Directions:** Given the promising results, further research is recommended to explore the long-term durability and self-healing properties of Combretum exudates in real-world applications, as well as the potential for scaling up the extraction and application processes for broader industrial use.

REFERENCES

- Abd El Maksoud, S., Fouda, A. E. A., & Badawy, H. (2024). Furosemide drug as a corrosion inhibitor for carbon steel in 1.0 M hydrochloric acid. *Scientific Reports*, 14, 9052. <https://doi.org/10.1038/s41598-024-48557-3>
- Al-Amiery, A. A., Isahak, W. N. R. W., & Al-Azzawi, W. K. (2023). Corrosion inhibitors: Natural and synthetic organic inhibitors. *Lubricants*, 11(174). <https://doi.org/10.3390/lubricants11030174>
- Al-Amiery, A. A., Yousif, E., Isahak, W. N. R. W., & Al-Azzawi, W. K. (2023). A review of inorganic corrosion inhibitors: Types, mechanisms, and applications. *Tribology International*, 45, 313–339. <https://doi.org/10.1016/j.triboint.2023.106790>
- Alkadir Aziz, I. A., Annon, I. A., Abdulkareem, M. H., Hanoon, M. M., Alkaabi, M. H., Shaker, L. M., Alamiery, A. A., Wan Isahak, W. N., & Takriff, M. S. (2021). Insights into corrosion inhibition behaviour of a 5-mercapto-1,2,4-triazole derivative for mild steel in hydrochloric acid solution: Experimental and DFT studies. *Lubricants*, 9(122). <https://doi.org/10.3390/lubricants9040122>
- Chigondo, M., & Chigondo, F. (2016). Recent natural corrosion inhibitors for mild steel: An overview. *Journal of Chemistry*. <https://doi.org/10.1155/2016/6208937>
- Dawood, M. A., Alasady, Z. M. K., Abdulazeez, M. S., Ahmed, D. S., Sulaiman, G. M., Kadhum, A. A. H., Shaker, L. M., & Alamiery, A. A. (2021). The corrosion inhibition effect of a pyridine derivative for low carbon steel in 1 M HCl medium: Complemented with antibacterial studies. *International Journal of Corrosion and Scale Inhibition*, 10(1766–1782). <https://doi.org/10.17675/2305-6894-2021-10-4-4>
- Dawood, M. A., Alasady, Z. M. K., Abdulazeez, M. S., Ahmed, D. S., Sulaiman, G. M., Kadhum, A. A. H., Shaker, L. M., & Alamiery, A. A. (2021). The corrosion inhibition effect of a pyridine derivative for low carbon steel in 1 M HCl medium: Complemented with antibacterial studies. *International Journal of Corrosion and Scale Inhibition*, 10, 1766–1782. <https://doi.org/10.17675/2305-6894-2021-10-4-4>
- E Abd El Maksoud, S., Fouda, A. E. A., & Badawy, H. (2024). Furosemide drug as a corrosion inhibitor for carbon steel in 1.0 M hydrochloric acid. *Scientific Reports*, 14, 9052. <https://doi.org/10.1038/s41598-024-48557-3>
- Fawzy, A., Abdallah, M., Zaafarany, I., Ahmed, S., & Althagafi, I. (2022). Thermodynamic, kinetic and mechanistic approach to the corrosion inhibition of carbon steel by new synthesized amino acids-based surfactants as green

- inhibitors in neutral and alkaline aqueous media. *Journal of Molecular Liquids*, 265, 276–291. <https://doi.org/10.1016/j.molliq.2018.12.032>
- Hameed, R. S., Aleid, G., Ragab, H., Alshafey, H., Aljuhani, E., & Almhyawi, S. (2024). Green synthesis of polymeric surfactants from recycling of plastic waste for applications on steel protection in the petroleum industry. *Green Chemistry Letters and Reviews*, 17, 2379442. <https://doi.org/10.1080/17518253.2024.2379442>
 - Harsimran, S., Santosh, K., & Rakesh, K. (2021). Overview of corrosion and its control: A critical review. *Proceedings of Engineering Science*, 3, 13–24. <https://doi.org/10.1016/j.proeng.2021.01.003>
 - Hu, K., Zhuang, J., Zheng, C., Ma, Z., Yan, L., Gu, H., Zeng, X., & Ding, J. (2016). Effect of novel cytosine-l-alanine derivative based corrosion inhibitor on steel surface in acidic solution. *Journal of Molecular Liquids*, 222, 109–117. <https://doi.org/10.1016/j.molliq.2016.07.024>
 - Iorhuna, F. (2024). Itraconazole drug as corrosion inhibitor for aluminium in 0.7 M hydrochloric acid medium. *Journal of Materials and Environmental Science*, 15, 501–511. <https://doi.org/10.26872/jmes.2024.15.5.501>
 - Kadhum, A., Betti, N., Al-Adili, A., Shaker, L., & Al-Amiry, A. (2022). Limits and developments in organic inhibitors for corrosion of mild steel: A critical review (Part two: 4-aminoantipyrine). *International Journal of Corrosion and Scale Inhibition*, 11, 43–63. <https://doi.org/10.17675/2305-6894-2022-11-1-3>
 - Koch, G. (2017). Cost of corrosion. In *Trends in oil and gas corrosion research and technologies* (pp. 3–30). Woodhead Publishing. <https://doi.org/10.1016/B978-0-08-100732-0.00001-3>
 - Liu, D., Jia, R., Xu, D., Yang, H., Zhao, Y., Khan, M. S., Huang, S., Wen, J., Yang, K., & Gu, T. (2019). Biofilm inhibition and corrosion resistance of 2205-Cu duplex stainless steel against acid producing bacterium *Acetobacter acetii*. *Journal of Materials Science and Technology*, 35, 2494–2502. <https://doi.org/10.1016/j.jmst.2019.05.020>
 - NACE. (2025). NACE study estimates global cost of corrosion. Retrieved from <https://www.rustbullet.com/cost-of-corrosion/?srsltid=AfmBOoor60Cy-USkAyUAObxGazC-ThrGmbPpliLgqczvovNQZCWmvT-Q>
 - Oubahou, M., el Aloua, A., Benzbiria, N., Harrari, S., Takky, D., Youssef, N., Zeroual, A., Wang, S.-F., Syed, A., & Belghiti, M. E. (2024). Electrochemical, thermodynamic and computational investigation of the use of an expired drug as a sustainable corrosion inhibitor for copper in 0.5 M H₂SO₄. *Materials Chemistry and Physics*, 323, 129642. <https://doi.org/10.1016/j.matchemphys.2024.129642>
 - Putra, R., Muhammad, A., Huzni, S., & Fonna, S. (2020). Expecting of corrosion rate in a material affected by differences soil type in controlled environments. *Materials & Corrosion Engineering Management*, 1(2), 31–34. <https://doi.org/10.3390/ma102031>
 - Sharma, S., Solanki, A. S., Thakur, A., Sharma, A., Kumar, A., & Sharma, S. K. (2024). Phytochemicals as eco-friendly corrosion inhibitors for mild steel in sulfuric acid solutions: A review. *Corrosion Reviews*, 42(727–742). <https://doi.org/10.1515/corrrev-2023-0170>
 - Timothy, U., Umoren, P., Solomon, M., Igwe, I., & Umoren, S. (2023). An appraisal of the utilization of natural gums as corrosion inhibitors: Prospects, challenges, and future perspectives. *International Journal of Biological Macromolecules*, 253, 126904. <https://doi.org/10.1016/j.ijbiomac.2023.126904>
 - Verma, C., Ebenso, E. E., & Al-Moubaraki, A. (2021). Recent developments in sustainable corrosion inhibitors: Design, performance, and industrial scale applications. *Materials Advances*, 2, 3806–3850. <https://doi.org/10.1039/D1MA00021H>
 - Wang, X., Yang, J., Chen, X., Liu, C., & Zhao, J. (2022). Synergistic inhibition properties and microstructures of self-assembled imidazoline and phosphate ester mixture for carbon steel corrosion in the CO₂ brine solution. *Journal of Molecular Liquids*, 357, 119140. <https://doi.org/10.1016/j.molliq.2022.119140>
 - Zhao, J., van Ommen, J. R., & Garcia, S. J. (2024). Gas-phase deposited nanolayers guard organic microparticles in polymer matrices for active corrosion protection at damages. *Progress in Organic Coatings*, 192, 108522. <https://doi.org/10.1016/j.porgcoat.2024.108522>
 - Zunita, M., & Rahmi, V. A. (2023). Advancement of plant extract/ionic liquid-based green corrosion inhibitor. *Chemistry Africa*, 7, 505–538. <https://doi.org/10.1007/s42250-023-00494-5>